



Minerva Access is the Institutional Repository of The University of Melbourne

Author/s:

Karami, S;TALEI, M;Hawkes, ER;Yu, H

Title:

Lewis number effects on edge-flame propagation in lifted turbulent flames

Date:

2015

Citation:

Karami, S., TALEI, M., Hawkes, E. R. & Yu, H. (2015). Lewis number effects on edge-flame propagation in lifted turbulent flames. Yang, Y (Ed.) Smith, N (Ed.) Proceedings of the Australian Combustion Symposium 2015, pp.300-303. The Combustion Institute Australia & New Zealand Section.

Persistent Link:

<https://hdl.handle.net/11343/258645>

Lewis number effects on edge-flame propagation in lifted turbulent flames

Shahram Karami^{1,*}, Mohsen Talei², Evatt R. Hawkes^{1,3}, Hongfeng Yu⁴

¹ School of Photovoltaic and Renewable Energy

The University of New South Wales, NSW 2052, Australia

² Department of Mechanical Engineering

University of Melbourne, Melbourne, VIC 3010, Australia

³ School of Mechanical Engineering

The University of New South Wales, NSW 2052, Australia

⁴ Computer Science and Engineering

University of Nebraska-Lincoln, Lincoln, NE 68588, United States of America

Abstract

Three turbulent lifted slot-jet flames of different fuel Lewis numbers are studied using direct numerical simulation (DNS). To reduce the computational cost, a one-step chemistry model is employed with a mixture-fraction dependent activation energy reproducing the dependence of the laminar flame speed on the equivalence ratio which is representative of hydrocarbon fuels. In addition to turbulent flames, axisymmetric laminar jet flames with a same chemistry model to that of turbulent flames are simulated. It is found that the maximum reaction rate decreases as the Lewis number increases in the laminar cases. Analysis of the turbulent cases reveals that the extinction limit is affected by the Lewis number of the fuel. The scalar dissipation rate of the extinction limit increases as the Lewis number decreases. For a given positive curvature, the conditional edge-flame propagation velocity on the curvature increases as the Lewis number decreases. This is similar to the observation in premixed flames and can be explained based on thermo-diffusive effects.

Keywords: Turbulent lifted flames, Lewis Number, Edge-flames, Triple flames.

1. Introduction

Recently, we are witnessing a global movement towards using alternative and cleaner fuels to produce energy. One of the challenges with these fuels such as syngas and hydrogen is the possible impacts of thermo-diffusive instabilities on the combustion efficiency and pollutant emissions. The non-dimensional number describing this effect is known as Lewis number which is defined as the ratio of thermal diffusivity to molecular diffusivity. It is well-known that the propagation velocity of a laminar premixed flame depends on the Lewis number of reactants and the flame front curvature [1]. For triple flames, the curvature of the flame front is dominantly positive which means the flame structure is convex towards reactant, therefore it is expected to observe a higher propagation velocity for triple flames with increasing the fuel Lewis number [2-4]. This can be explained based on heat and species diffusion. When the flame front is convex towards the reactant and the Lewis number is smaller than unity, the reactants will diffuse into the reaction zone more rapidly than the heat diffused away from this region. Consequently, the temperature will increase, resulting in a rapid increase of the reaction rate [4]. Chen et al. [5] studied the effect of Lewis number in a counter flow and a laminar lifted flame configuration. The methane- and propane-air flames with different dilution levels in the fuel stream, facilitating a wide range of fuel Lewis number, were studied. They reported that the reactant effective Lewis number at the

flame base is an important parameter in the counter-flow configuration whereas the fuel Lewis number is important in lifted triple flames.

The importance of the Lewis number has been also investigated in turbulent premixed [6-9] and non-premixed flames [10]. The experimental studies of lifted turbulent non-premixed flames [11] have also investigated the effects of the fuel Lewis number on the stabilisation process. Cessou et. al. [11] found that the lifted height and the blow-out limit of hydrocarbon fuels depend on the Lewis number.

It is very challenging to measure the edge-flame propagation velocity, curvature of the flame front and scalar dissipation rate simultaneously in experimental setups. However, this simultaneous measurement is required to understand the edge-flame dynamics in lifted flames in addition to the stabilization mechanism. Therefore, this paper seeks to address this gap by analysing the response of the flame propagation and flame front curvature to the scalar dissipation rate as a key parameter in this problem when the fuel Lewis number of fuel varies.

2. Numerical method and simulation parameters

The non-dimensionalised conservation equations of mass, momentum, sensible energy and species are solved. These equations are non-dimensionalised with respect to the inlet jet width, H , the speed of sound, temperature and thermodynamic properties on the jet centreline at the inlet. A single-step irreversible reaction

* Corresponding author:
Phone: (+61) 2 9385 4602
Email: s.karami@unsw.edu.au

of $F+rO \rightarrow (1+r)P$ where r is the stoichiometric ratio, i.e. the mass of oxidant disappearing with unit mass of fuel was used. The DNS code S3D_SC [12] is employed here. The solver uses high-order accurate, low dissipative numerical schemes and a 3D structured, Cartesian mesh. The spatial derivatives were discretised using an 8th order central differencing scheme and the time integration was performed with a 6-stage, 4th order, explicit Runge-Kutta method. To suppress the numerical fluctuations at high wave numbers, a 10th order filter was applied every 10 time steps. Non-reflecting outflow boundary conditions were used in the streamwise and transverse directions, and periodic boundary conditions were applied in the spanwise direction. The simulation parameters along with their values are presented in table 1. The configuration is a slot jet flame. The mean inlet axial velocity, U_{in} , and fuel mass fraction, Y_F , were specified using a tanh-based profile with an inlet momentum (and mixing layer) thickness, δ , is equal to $0.05H$. To describe the velocity fluctuations at the inlet, a homogeneous isotropic turbulence field based on a prescribed turbulent energy spectrum with a turbulence intensity of 5% is first produced. These velocity fluctuations are then added to the mean inlet velocity using the Taylor's frozen turbulence hypothesis [12, 13].

A uniform grid spacing of $0.02H$ was chosen for the streamwise and spanwise directions. An algebraically stretched mesh was applied [14] in the transverse direction which maintained uniform spacing of $0.02H$ in $|y| < 7.5H$ and less than 3% of grid stretching in the region of $|y| > 7.5H$. The simulation was run for 18.0 jet flow through times, $t_j = L_x/U_j$ (where L_x is the length of the computational domain in the streamwise direction), and the data of the last $12.0t_j$ were used for analysis. The simulations were performed for three different Lewis numbers of the fuel as 0.7, 1.0 and 1.3. The turbulence and chemistry resolutions are discussed in more details in Ref. [12].

Table 1 Numerical and physical parameters of the simulation.

Description	Value
Domain size ($L_x \times L_y \times L_z$)	$16H \times 24H \times 6H$
Number of grid points ($N_x \times N_y \times N_z$)	$800 \times 800 \times 300$
Mean inlet jet Mach number (U_j/a_{ref})	0.48
Laminar co-flow Mach number (U_{co}/a_{ref})	0.001
Jet non-dimensional temperature (T_{jet})	2.5
Co-flow non-dimensional temperature ($T_{co-flow}$)	2.5
Jet Reynolds number (Re)	5280
Inlet velocity fluctuation intensity	5%
Fuel mass fraction in the fuel stream ($Y_{F,o}$)	1.0
Oxidiser mass fraction in the oxidiser stream ($Y_{O,o}$)	0.233
Stoichiometric oxidiser to fuel mass ratio (r)	4.0
Heat-release parameter (α)	0.86
Zel'dovich number (β)	5.0
Non-dimensionalisation Damköhler number (Da)	800
Lewis number (Le)	0.7 – 1.0 – 1.3
Prandtl number (Pr)	0.7

3. Mathematical background

Three components of the flow velocity in a time-resolved manner have been measured simultaneously by the most advanced experiments [15]. These have provided very useful information; however, flame propagation velocities relative to the flow have never

been measured. In our previous study of stabilization mechanism of a turbulent lifted flame with unity Lewis number of the fuel, it was shown that flame propagation plays a key role, in the stabilization process. However, to the best of our knowledge, there is no study on the effects of the fuel Lewis number on the edge-propagation velocity in lifted flames. Therefore, this study will focus on Lewis number effects in turbulent lifted flames. For this purpose, the flame edge is defined as the intersection of a mixture-fraction iso-surface with a product mass-fraction iso-surface. The mixture-fraction iso-values were 0.077, 0.07 and 0.066 which correspond to the mixture-fractions having the highest laminar flame speeds in one-dimensional flat premixed laminar flames with the Lewis numbers of 0.7, 1.0 and 1.3, respectively. The product iso-values were selected at the point of the maximum reaction rate for each laminar flame corresponding to a given Lewis number.

The edge-flame displacement speed, S_e , in the plane of the mixture-fraction iso-surface in the direction T_2 , which is the tangent vector to the mixture-fraction iso-surface that is normal to the intersection line which defines the edge, pointing towards the unburned reactants is given in terms of the product mass-fraction self-displacement speed S_d , the mixture-fraction self-displacement speed S_z , and the inner product of the normal vectors to product and mixture-fraction iso-surfaces k as [16]:

$$S_e^* = \frac{S_d^* - kS_z^*}{\sqrt{1 - k^2}} \quad (1)$$

The iso-surface self-displacement speeds are given by [17]:

$$\rho_u S_z^* = \rho S_z = \frac{1}{|\nabla Z|} \left(-\frac{\partial}{\partial x_j} \left(\frac{\mu}{ScRe} \frac{\partial Z}{\partial x_j} \right) \right), \text{ and} \quad (2)$$

$$\rho_u S_d^* = \rho S_d = \frac{1}{|\nabla Z|} \left(-\dot{\omega}_P - \frac{\partial}{\partial x_j} \left(\frac{\mu}{ScRe} \frac{\partial Y_P}{\partial x_j} \right) \right),$$

The curvature of product mass fraction iso-surfaces is defined as $|\nabla \cdot \mathbf{N}_{Y_P}|$. Figure 1 presents schematic of the edge-flame propagation velocity.

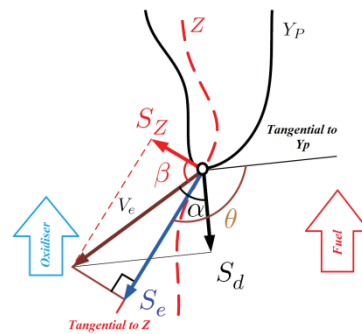


Figure 1. Schematic of the edge-propagation velocity.

4. Results

For an orientation first, symmetric laminar lifted flames with the same chemistry parameters to those of turbulent flames were simulated. Figure 2 shows the reaction rates of laminar triple flames for different fuel

Lewis numbers. It is observed that the maximum reaction rates decreases as the Lewis number increases which is expected as the curvature is positive [18]. Also it is noted that the lifted height increases and the diffusion tail disappears as the Lewis number increases.

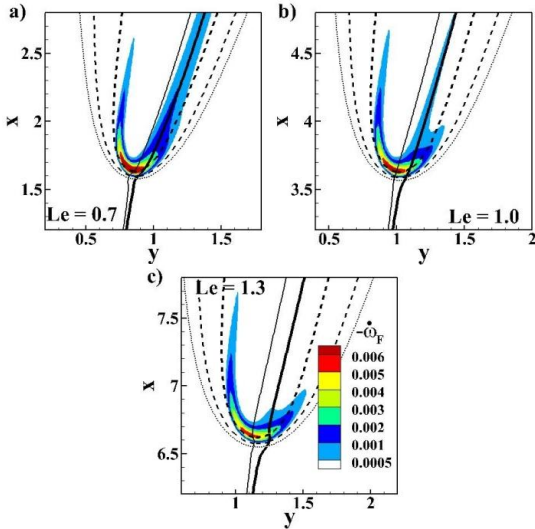


Figure 2. The contour plots of reaction rates of laminar triple flames with fuel Lewis number of a) 0.7, b) 1.0 and c) 1.3 (The solid lines are mixture fraction iso-lines and the dashed lines are different levels of product mass fraction).

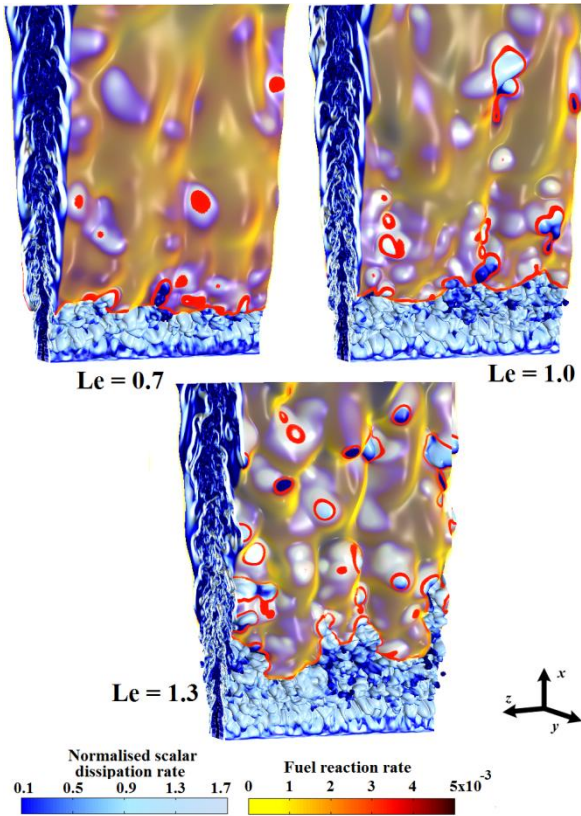


Figure 3. Three-dimensional volume rendering of logarithm of the scalar dissipation rate (blue/white) and reaction rate (red/orange) for different Lewis number of fuels.

Moving to the turbulent cases, Fig. 3 presents the volume rendering of logarithm of the scalar dissipation rate (blue/white) and reaction rate (red/orange) for different Lewis numbers of the fuel stream. From left to right are cases with the Lewis numbers of 0.7, 1.0 and 1.3. The reaction sheet is strongly positive for $Le = 0.7$

but becomes weaker as the Lewis number increases. The flame base also experiences a higher level of distortion. As the Lewis number increases, the shield generated by the flame becomes weaker and therefore the probability of being broken by large-eddy structures is higher. As a result, more holes are observed for $Le = 1.3$. Also, it is noted that the holes are highly convoluted for this case.

The roles of the scalar dissipation rate and curvature are now discussed. Figure 4 shows the conditional mean of the edge-propagation velocity on the scalar dissipation rates for different Lewis numbers. The results are consistent with those observed with regards to the triple flame response to the scalar dissipation rate [2, 4, 19-21]. The edge-flame propagation velocity decreases as the scalar dissipation rate increases and the flame is extinguished at a critical value. However, the extinction limits are different for different cases. The $Le = 0.7$ case has a higher extinction limit and a higher propagation velocity for all values of scalar dissipation rates. On the other hand, the extinction limit for $Le = 1.3$ is the smallest. This implies that the flame with a higher Lewis number will be extinguished more easily. This is in agreement with the observation in the literature that the critical scalar dissipation rate marking the triple flame extinction increases as the Lewis number decreases [4, 22, 23]. Furthermore, this explains formation of a larger number of local extinctions on the flame sheet and a higher convolution at the flame base for $Le > 1$ observed in Fig. 3.

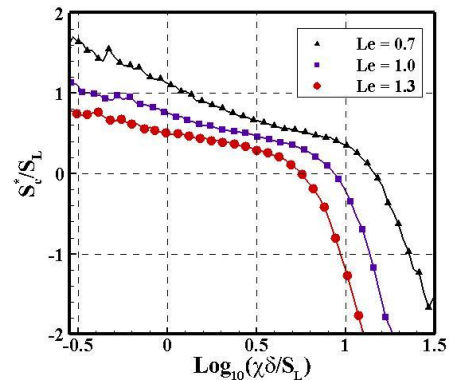


Figure 4. Conditionally averaged edge-propagation velocity on normalised scalar dissipation rate at the flame base for three cases of Lewis number 0.7, 1.0 and 1.3.

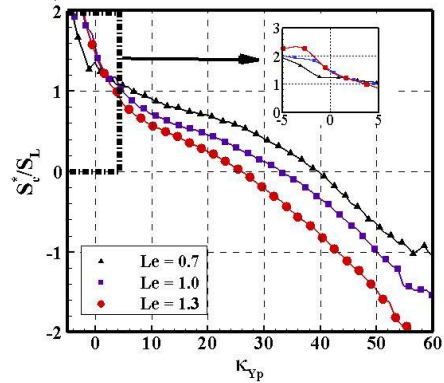


Figure 5. Conditionally averaged edge-propagation velocity on product-mass fraction curvature at the flame base for three cases of Lewis number 0.7, 1.0 and 1.3.

Another important parameter is the flame front curvature which has been shown to play an important role in flame propagation [7, 8]. Figure 5 presents the

conditional mean of the edge-flame propagation velocity on the curvature of the product mass-fraction iso-surface. In contrast to laminar triple flames, there is a small region of negative curvatures which is due to the effects of turbulence. The edge-flame propagation velocity non-linearly decreases as the curvature increases. It is well-known that a higher scalar dissipation rate causes a larger curvature and consequently two premixed flames merge on the diffusion tails [24]. This is consistent with what is observed in Fig. 5 as high scalar dissipation rates are coincident with large curvatures. Figure 5 also shows that for a given positive curvature, the edge propagation velocity increases as Lewis number of the fuel decreases. This observation can be explained using the thermo-diffusive properties of the fuel. When the curvature is positive and $Le < 1$, the fuel diffuses faster into the flame front than the heat diffusing out. This will increase the reaction rate and therefore the edge-propagation velocity. The opposite behaviour is however expected for $Le > 1$.

5. Conclusion

Direct numerical simulation (DNS) was used to study the effects of fuel Lewis number on the edge-flame propagation in laminar and turbulent lifted flames. It was found that the maximum reaction rate decreases as the Lewis number increases in the laminar cases. For the turbulent cases, an increased number of extinction holes and more distortion of the flame base were observed as the Lewis number was increased. In contrast to laminar triple flames in which the curvatures of the flame fronts are positive, negative curvatures were also observed at the flame base of the turbulent cases. It was observed that the edge-flame propagation velocity of the fuel with $Le < 1$ is higher than other cases for all values of the scalar dissipation rate when the curvature of the product mass-fraction is positive. This is similar to effects of Lewis number observed in premixed flames.

4. Acknowledgments

This work was supported by the Australian Research Council (ARC). The research was also supported by access to computational resources on the Australian NCI National Facility through the National Computational

Merit Allocation Scheme and Intersect Australia partner share.

5. References

- [1] P. A. Libby, A. Liñán, F. A. Williams, *Combust. Sci. Technol.* **34** (1-6) (1983), pp. 257-293.
- [2] J. Daou, F. Al-Malki, *Combust. Theor. Model.* **14** (2) (2010), pp. 177-202.
- [3] R. Daou, J. Daou, J. Dold, *Combust. Theor. Model.* **8** (4) (2004), pp. 683-699.
- [4] J. Daou, A. Liñán, *Combust. Theor. Model.* **2** (4) (1998), pp. 449-477.
- [5] R. H. Chen, M. Chaos, A. Kothawala, *Proc. Combust. Inst.* **31** (1) (2007), pp. 1231-1237.
- [6] A. J. Aspden, M. S. Day, J. B. Bell, *J. Fluid Mech.* **680** (2011), pp. 287-320.
- [7] A. J. Aspden, M. S. Day, J. B. Bell, *Proc. Combust. Inst.* **33** (1) (2011), pp. 1463-1471.
- [8] A. J. Aspden, M. S. Day, J. B. Bell, *Proc. Combust. Inst.* **33** (1) (2011), pp. 1473-1480.
- [9] J. B. Bell, R. K. Cheng, M. S. Day, I. G. Shepherd, *Proc. Combust. Inst.* **31** (1) (2007), pp. 1309-1317.
- [10] H. Hesse, N. Chakraborty, E. Mastorakos, *Proc. Combust. Inst.* **32** (1) (2009), pp. 1399-1407.
- [11] A. Cessou, C. Maurey, D. Stepowski, *Combust. Flame* **137** (4) (2004), pp. 458-477.
- [12] S. Karami, E. R. Hawkes, M. Talei, J. H. Chen, *J. Fluid Mech.* **777** (2015), pp. 633-689.
- [13] C. S. Yoo, R. Sankaran, J. H. Chen, *J. Fluid Mech.* **640** (2009), pp. 453-481.
- [14] E. R. Hawkes, O. Chatakonda, H. Kolla, A. R. Kerstein, J. H. Chen, *Combust. Flame* **159** (8) (2012), pp. 2690-2703.
- [15] I. Boxx, C. Heeger, R. Gordon, B. Böhm, A. Dreizler, W. Meier, *Combust. Flame* **156** (1) (2009), pp. 269-271.
- [16] E. Hawkes, R. Sankaran, J. Chen, 16th Australasian Fluid Mechanics Conference (AFMC) (2007), pp. 1271-1274.
- [17] S. B. Pope, *Int. J. Eng. Sci.* **26** (5) (1988), pp. 445-469.
- [18] J. Buckmaster, M. Matalon, *Symp. (Int.) Combust.* **22** (1) (1989), pp. 1527-1535.
- [19] J. Boulanger, L. Vervisch, J. Reveillon, S. Ghosal, *Combust. Flame* **134** (4) (2003), pp. 355-368.
- [20] V. Favier, L. Vervisch, *Combust. Flame* **125** (1-2) (2001), pp. 788-803.
- [21] S. Ghosal, L. Vervisch, *J. Fluid Mech.* **415** (2000), pp. 227-260.
- [22] M. Matalon, *Proc. Combust. Inst.* **32** (1) (2009), pp. 57-82.
- [23] M. Matalon, *Combust. Sci. Technol.* **31** (3-4) (1983), pp. 169-181.
- [24] I. A. Mulla, S. R. Chakravarthy, *Combust. Flame* (2014), pp.